The 2017 World Congress on
Advances in Structural Engineering and Mechanics (ASEM17)
28 August - 1 September, 2017, Ilsan(Seoul), Korea

The evaluation of building behavior near soil slopes

Mohammad Mahdi Aminpour[*1] and Mohammad Maleki[2]

[1, 2] *Department of Civil Engineering, Bu-Ali Sina University, Hamedan, I.R. Iran*
[1)] aminpour.geoeng@gmail.com

ABSTRACT

Many buildings are constructed near the soil slopes. Such structures can be regarded as an extra surcharge on the slopes. The intensity and location of the surcharge affects the slopes. In this research, using limit analysis method and upper bound theory with non-associated flow rule, the building behavior near soil has been estimated. The authors have suggested a formulation for calculating the velocity behavior of the soil slope in presence of a surcharge for different failure modes. The effects of building's intensity, location of building as well as the soil properties have been investigated.

1. INTRODUCTION

There have been various studies on surcharge near the slope. In analytical studies, the kinematic theorem of limit analysis presented by Michalowski (2007), Askari and Farzaneh (2003), Mojallal et al. (2012), Aminpoor and Ghanbari (2014), Yu et al. (2014), Zhang et al. (2016) that investigated different condition for slope stability, slope displacement and surcharge near the slope. The limit equilibrium technique presented by Cai and Bathurst (1996), Huang and Wang (2005), Huang and Wu (2006, 2007), Huang and Wu (2009), Caltabiano et al. (2012).

Among the experimental studies, following works can be mentioned: Huang et al. (2008, Bathurst et al. (2009), Huang and Luo (2010), Huang et al. (2011), Bathurst et al. (2012) and Srilatha et al. (2013). Numerical studies include those by Liu (2009), Lee et al. (2010), Liu and Wang (2011).

In the present research, using limit analysis method, the yield surcharge building near the slope has been studied. The rotational failure modes has been considered in this research. Finally, this failure mode has been compared with the limit equilibrium method.

[1] Ph.D. Student
[2] Associate Professor

2. YIELD CRITERION

Davis (1968) by examining the failure mechanism on slip-lines for a non-associated Mohr Coulomb material, established that the shear and normal stress are related by

$$\tau = \sigma_n \tan\phi^* + c^* \tag{1}$$

Where c^* and ϕ^* are 'reduced' strength parameters, defined by

$$\left.\begin{aligned} c^* &= \beta c \\ \tan\phi^* &= \beta \tan\phi \end{aligned}\right\} \quad \beta = \frac{\cos\psi \cos\phi}{1-\sin\psi \sin\phi} \tag{2}$$

c is the cohesion, ϕ is the friction angle and ψ is the dilation angle. The use of these reduced strengths provides a practical means for non-associated flow rule in limit analysis (Sloan 2013). The new CJS yield criteria was presented in 1988 by Cambo, Jafari and Seidoroff at the French School of French Lion to express the behavior of the soil soils. The dependence of the rupture level is considered to be the invariant of the stress tensor and non-associated flow rule is considered. In general, this model has a deformation level as follows (Maleki 1998):

$$f(\sigma) = s_{II} h(\theta) - R_m I_1 = 0 \tag{3}$$

$$s_{II} = \sqrt{s_{ij}\, s_{ij}}$$

$$s_{ij} = \sigma_{ij} - \frac{\sigma_{kk}}{3}\delta_{ij}$$

$$I_1 = \sigma_{kk}$$

Where Rm is the radius of failure and $h(\theta)$ control the variation of the failure radius in the deviation plan (Maleki 1998).

$$h(\theta) = (1-\gamma\cos 3\theta)^{1/6} = \left[1 - \sqrt{54}\,\gamma\,\frac{\det(s_{ij})}{s_{II}^3}\right]^{1/6} \tag{4}$$

$$\cos 3\theta = \left[\frac{3\sqrt{3}}{2}\frac{J_3}{J_2^{3/2}}\right], \quad J_2 = \frac{1}{2}s_{ij}s_{ij}, \quad J_3 = \det(s_{ij})$$

With the approximation of the relation cjs and non-associated Mohr Coulomb, we find the following relation:

$$R_m = 2\sqrt{\frac{2}{3}}\,\frac{(1-\gamma)^{1/6}\sin\phi^*}{3-\sin\phi^*} \tag{5}$$

$$\left(\frac{1-\gamma_{cjs}}{1+\gamma_{cjs}}\right)=\left(\frac{3-\sin\phi^*}{3+\sin\phi^*}\right)^6 \tag{6}$$

3. Studying the failure mechanism

A slope is located next to a building (Fig. 1). For the rotational failure as illustrated in Fig. 1, the soil wedge rotates around the point O with the angular velocity ω. In this figure, X is the width of the failure wedge, a is the distance of surcharge from the edge of the slope, b is the width of the surcharge and hq is the height of the surcharge. The formula for the log-spiral failure surface can be expressed by Eq. (7). In this equation, $r(\theta)$ is the radius as a function of the arbitrary angle and $V(\theta)$ is the incipient velocity as a function of $r(\theta)$.

$$r(\theta)=r_0\exp\left[(\theta-\theta_0)\tan\varphi^*\right] \tag{7}$$

It has to be noted that the failure surface moves along the heel of the slope and can be located either in front of or behind the reinforced area. By considering non cohesion material, the rate of internal work is zero. The rate of work done by body forces can be obtained from Eq. (8) regardless of the location of the surcharge. In this equation, the functions f_1 to f_6 are dependent on h * and parameter. These functions have been introduced by other researchers (Crespellani et al. 1998; Michalowski 1998) and are summarized in the appendix.

$$\dot{W}=\gamma r_0^{\,3}\omega(f_1-f_2-f_3) \tag{8}$$

$$\varphi^*=\sin^{-1}\left(\frac{3R_m}{R_m+2\sqrt{\frac{2}{3}}(1-\gamma)^{1/6}}\right) \tag{9}$$

In order to calculate the minimum rate of external work due to the surcharge, three different cases of surcharge's location have been considered as following:

1- Case 1: The surcharge is completely located within the failure wedge
2- Case 2: The surcharge is partially located within the failure wedge
3- Case 3: The surcharge is completely located outside the failure wedge.

Considering the forces applied to the failure wedge and the length of their arms from the center of rotation, the rate of external work due to the surcharge for case 1 can be calculated by Eq. (10).

$$\dot{Q}=qb\left(r_0\cos\theta_0-X+a+\frac{b}{2}\right)\omega \tag{10}$$

In this equation $\bar{h}_q$ is the height of the center of mass of the building (surcharge) and X is the width of the failure wedge (Fig. 1). The rate of external work due to surcharge in case 2 is obtained from Eq. (11). It has to be noted that in case 3, since the surcharge is located outside the failure wedge, the rate of external work is zero.

$$\dot{Q} = q(X-a)\left(r_0\cos\theta_0 - \frac{X-a}{2}\right)\omega \tag{11}$$

Assuming at the time of failure, the rates of internal and external work can be equaled.

$$\dot{W} + \dot{Q} = 0 \tag{12}$$

Solving Eq. (12), the yield surcharge for the three cases of surcharge can be obtained from Eqs. (13) and (14). It has to be mentioned that the value of ω will be canceled out from the denominator and numerator of these equations.

In case 1:

$$q = \frac{-\gamma r_0^{\,3}(f_1 - f_2 - f_3)}{b\left(r_0\cos\theta_0 - X + a + \frac{b}{2}\right)} \tag{13}$$

In case 2:

$$q = \frac{-\gamma r_0^{\,3}(f_1 - f_2 - f_3)}{(X-a)\left(r_0\cos\theta_0 - \frac{X-a}{2}\right)} \tag{14}$$

In case 3 the surcharge has no effect to the slope. The yield surcharge is a function of two parameters and $_h$. By solving the obtained equations and Eq. (15) simultaneously, the critical yield surcharge can be calculated.

$$\frac{\partial q}{\partial \theta_0} = \frac{\partial q}{\partial \theta_h} = 0 \tag{15}$$

4. The results of the suggested method

By decreasing the distance of surcharge, the yield condition becomes critical. As the distance of surcharge from the edge of the slope is increased again, the effect of surcharge is decreased. In this figure, the height of the center of mass of the building is 8 m and *b* is one meter. The soil and slope properties are shown in Table 1. Variations of yield surcharge versus distance of surcharge from the edge of slope for different widths are shown in Table 2.

Table 3 shows variations of the yield surcharge with different angles. The steeper slopes show smaller yield accelerations and larger displacements.

Table 4 shows a comparison between the results of the suggested formulation and the results of Meyerhof, Vesic and Hansen limit equilibrium methods. The results show a good agreement between the suggested method and the others methods reported data.

5. Conclusion

Using the upper bound theory of limit analysis a new formulation is presented in this research for calculating yield surcharge of building near the soil slopes. For this purpose rotational failure modes have been considered. In this method, the effect of location of surcharge related to the edge of the slope and soil properties such as internal friction angle of soil and specific weight of soil have been investigated. For the case where the surcharge has a small distance from the edge of the slope, the rotational mode would result in a critical manner. The reason is an increase in the arm of the moment induced by surcharge. Finally, by increasing the distance of surcharge from the edge of the slope the effect of surcharge disappears and the slope would behave similar to the case without a surcharge.

6. Appendix

The functions f_1 to f_6 are defined as following (Crespellani et al. 1998; Michalowski 1998).

$$f_1(\theta_0,\theta_h)=\frac{\left\{\left(3\tan\varphi\cos\theta_h+\sin\theta_h\right)\exp\left[3(\theta_h-\theta_0)\tan\varphi^*\right]-3\tan\varphi\cos\theta_0-\sin\theta_0\right\}}{3(1+9\tan^2\varphi^*)} \tag{16}$$

$$f_2(\theta_0,\theta_h)=\frac{1}{6}\frac{X}{r_0}\left(2\cos\theta_0-\frac{X}{r_0}\right)\sin\theta_0 \tag{17}$$

$$f_3=\frac{1}{6}\exp\left[(\theta_h-\theta_0)\tan\varphi^*\right]\left[\sin(\theta_h-\theta_0)-\frac{X}{r_0}\sin\theta_h\right]\times\left\{\cos\theta_0-\frac{X}{r_0}+\cos\theta_h\exp\left[(\theta_h-\theta_0)\tan\varphi^*\right]\right\} \tag{18}$$

$$f_4(\theta_0,\theta_h)=\frac{1}{3(1+9\tan^2\varphi^*)}\left\{\left(3\tan\varphi^*\sin\theta_h-\cos\theta_h\right)\exp\left[3(\theta_h-\theta_0)\tan\varphi^*\right]-3\tan\varphi^*\sin\theta_0+\cos\theta_0\right\} \tag{19}$$

$$f_5(\theta_0,\theta_h)=\frac{1}{3}\frac{X}{r_0}\sin^2\theta_0 \tag{20}$$

$$f_6(\theta_0,\theta_h)=\frac{1}{6}\exp\left[(\theta_h-\theta_0)\tan\varphi^*\right]\left[\sin(\theta_h-\theta_0)-\frac{X}{r_0}\sin\theta_h\right]\times\left\{\sin\theta_0+\sin\theta_h\exp\left[(\theta_h-\theta_0)\tan\varphi^*\right]\right\} \tag{21}$$

$$\frac{X}{r_0}=\frac{1}{\sin\theta_h}\left[\sin(\theta_h-\theta_0)-\frac{H}{r_0}\frac{\sin(\beta+\theta_h)}{\sin\beta}\right] \tag{22}$$

$$\frac{H}{r_0}=\sin\theta_h\exp\left[(\theta_h-\theta_0)\tan\varphi^*\right]-\sin\theta_0 \tag{23}$$

References

Aminpoor, M.M. and Ghanbari, A. (2014), "Design charts for yield acceleration and seismic displacement of retaining walls with surcharge through limit analysis", *Structural Engineering and Mechanics*, **52**(6), 1225-1256.

Askari, F. and Farzaneh, O. (2003), "Upper-bound solution for seismic bearing capacity of shallow foundations near slopes", *Ge´otechnique*, **53**(8), 697–702.

Bathurst, R.J., Nernheim, A., Walters, D.L., Allen, T. M., Burgess, P. and Saunders, D.D. (2009), "Influence of reinforcement stiffness and compaction on the performance of four geosynthetic-reinforced soil walls", *Geosynthetics International*, **16**(1), 43-59.

Bathurst, R.J., Hatami, K. and Alfaro, M.C. (2012), *Geosynthetic Reinforced Soil Walls and Slopes-Seismic Aspects. Handbook of Geosynthetic Engineering, 2nd edn, in: Shukla, S. K. (Ed).* ICE Publishing, London, pp. 317–363.

Cai, Z. and Bathurst, R. J. (1996), "Seismic induced permanent displacement of geosynthetic reinforced segmental retaining walls", *Canadian Geotechnical Journal*, **33**(6), 937–955.

Caltabiano, S., Cascone, E. and Maugeri, M. (2012), "Static and seismic limit equilibrium analysis of sliding retaining walls under different surcharge conditions", *Soil Dyn. Earthq. Eng*., **37**, 38-55.

Crespellani, T., Madai, C. and Vannucchi, G. (1998), "Earthquake destructiveness potential factor and slope stability", *Geotechnique*, **48**(3), 411–9.

Davis, E. H. (1968), *Theories of Plasticity and Failure of Soil Masses. In Soil mechanics: selected topics,* (ed. I. K. Lee), pp. 341–354. New York, NY, USA: Elsevier.

Huang, C.C. and Wang, W.C. (2005), "Seismic displacement charts for the performance-based assessment of reinforced soil walls", *Geosynthetics International,* **12**(4), 176–190.

Huang, C.C. and Wu, S.H. (2006), "Simplified approach for assessing seismic displacements of soil-retaining walls. Part I: Geosynthetic reinforced modular block walls", *Geosynthetics International*, **13**(6), 219–233.

Huang, C.C. and Wu, S.H. (2007), "Simplified approach for assessing seismic displacements of soil-retaining walls. Part II: Geosynthetic-reinforced walls with rigid panel facing", *Geosynthetics International*, **14**(5), 264–276.

Huang, C.C., Horng, J.C. and Charng, J.J. (2008), "Seismic stability of reinforced slopes: effects of reinforcement properties and facing rigidity", *Geosynthetics International,* **15**(2), 107–118.

Huang, C.C. and Wu, H.J. (2009), "Seismic displacement analyses for a reinforced soil wall considering progressive development of reinforcement force", *Geosynthetics International,* **16**(3), 222-234.

Huang, C.C. and Luo, W.M. (2010), "Behavior of cantilever and geosynthetic-reinforced walls on deformable foundations", *Geotextiles and Geomembranes,* **28**, 448-459.

Huang, C.C., Horng, J.C., Chang, W.J. and Chiou, J.S. (2011), "Dynamic behavior of reinforced walls -Horizontal displacement response", *Geotextiles and Geomembranes*, **29**, 257-267.

Lee, K.Z.Z., Chang, N.Y. and Ko, H.Y. (2010), "Numerical simulation of geosynthetic-reinforced soil walls under seismic shaking", *Geotextiles and Geomembranes*, **28**(4), 317-334.

Liu, H. (2009), "Analyzing the reinforcement loads of geosynthetic-reinforced soil walls subject to seismic loading during the service life", *Journal of Performance of Constructed Facilities ASCE*, **23**(5), 292-302.

Liu, H., Wang, X. and Song, E. (2011), "Reinforcement load and deformation mode of geosynthetic- reinforced soil walls subject to seismic loading during service life", *Geotextiles and Geomembranes,* **29**, 1-16.

Maleki, M. (1998), "Modelisation Hierarchisee du Comportement des Sols", Theses de Doctorat, Ecole Centrale de Lyon.

Michalowski, R.L. (1998), "Limit analysis in stability calculations of reinforced soil structures", *Geotextiles and Geomembranes*, **16**, 311-331.

Michalowski, R.L. (2007), "Displacement of multiblock geotechnical structures subjected to seismic excitation", *Journal of Geotechnical and Geoenvironmental Engineering ASCE*, **133** (11), 1432-1439.

Mojalla, M., Ghanbari, A. and Askari, F. (2012), "A new analytical method for calculating seismic displacements in reinforced retaining walls", *Geosynthetics International*, **19**(3), 212–231.

Sloan, S. W. (2013), "Geotechnical stability analysis", *Ge´otechnique,* **63**(7), 531–572.

Srilatha, N., Madhavi Latha, G. and Puttappa, C.G. (2013), "Effect of frequency on seismic response of reinforced soil slopes in shaking table tests", *Geotextiles and Geomembranes,* **36**, 27-32.

Yu, S.B., Merifield, R.S., Lyamin, A.V. and Fu, X.D. (2014), "Kinematic limit analysis of pullout capacity for plate anchors in sandy slopes", *Structural Engineering and Mechanics*, **51**(4).

Zhang, G., Tan, J., Zhang, L. and Xiang, Y. (2016), "Limit analysis of 3D rock slope stability with non-linear failure criterion", *Geomechanics and Engineering*, **10**(1).

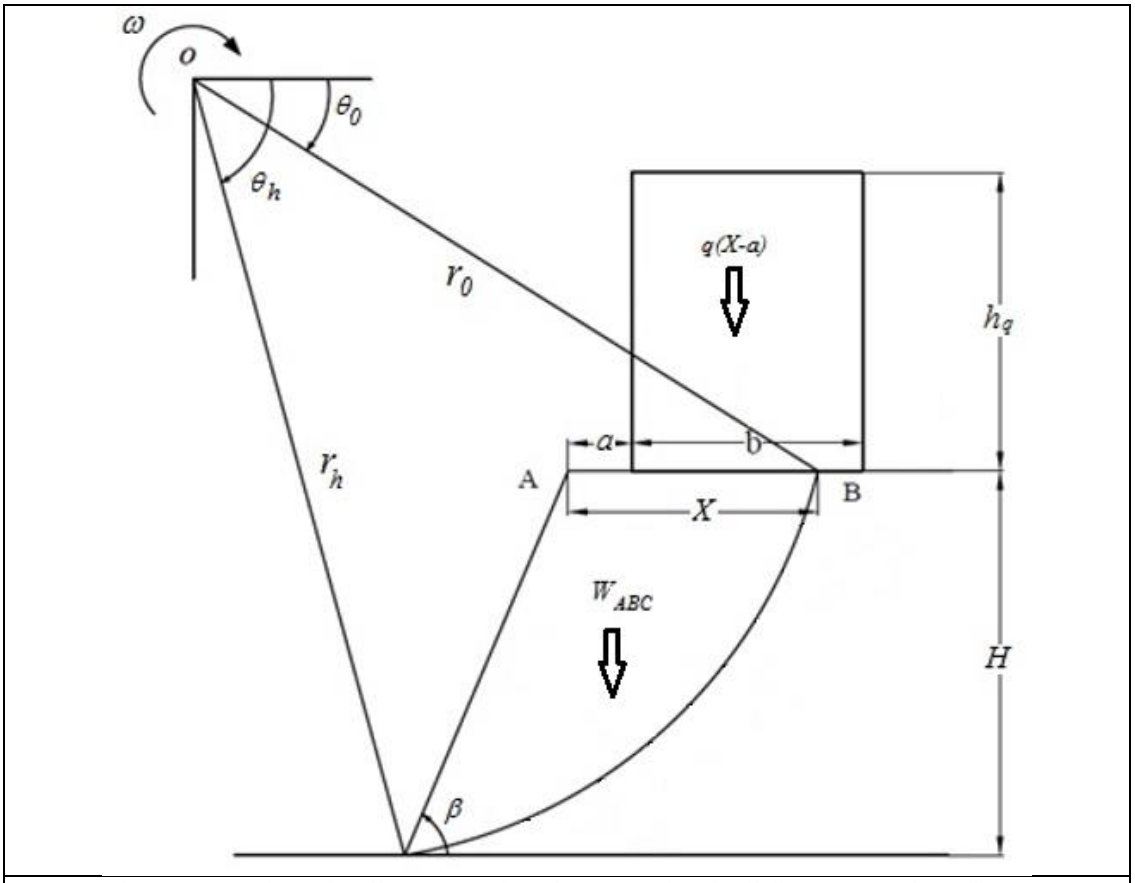

Fig. 1 Rotational failure mechanism for the building near the slope

Table 1. Soil and slope properties

b (m)	degrees	H (m)	R_m	(kN/m^3)	$_{CJS}$
1	30	5	0.320	18	0.863

Table 2. Variations of yield surcharge versus the distance of surcharge from the end of slope

a (m)	0	2 .5	5	10
q (Kpa)	415.34	618.24	779.68	783.31

Table 3. Variations of yield surcharge versus angles of slope

degrees	20	30	40
q (Kpa)	838.56	415.34	183.22

Table 4. Comparison of q values form suggested method and limit equilibrium methods

	Bearing capacity without slope			Bearing capacity near the slope			
a (m)	Meyerhof	Vesic	Hansen	Meyerhof	Vesic	Hansen	Proposed method
0	2119.117	2387.947	2246.467	379.178	427.2803	401.965	415.34